Journal of Advanced Biomedical Sciences

Journal of Advanced Biomedical Sciences
https://jabs.fums.ac.ir/
Online ISSN: 2783-1523

Fasa University of Medical Sciences

Biocompatibility Analysis of Mouse Spleen-Derived Extracellular Matrix

Yasin Ghabool[1], Mahshid Reghbati[1], Nasser Mahdavi-Shahri[2], Amin Tavassoli[3]

1. Department of Biology, Faculty of Sciences, Mashhad Branch, Islamic Azad University, Mashhad, Iran
2. Department of Biology, Faculty of Sciences, Ferdowsi University of Mashhad, Mashhad, Iran
3. Department of Biotechnology, Faculty of Veterinary Medicine, Ferdowsi University of Mashhad, Mashhad, Iran

Article Info

Article Type:
Research Article

Article history:
Received
27 Mar 2024
Received in revised form
11 May 2024
Accepted
29 May 2024
Published online
14 Jun 2024

Publisher
Fasa University of Medical Sciences

Abstract

Background & Objectives: This study aimed to construct a decellularized mouse spleen scaffold and evaluate its cellular compatibility *in vitro* using murine bone marrow-derived mesenchymal stem cells (BM-MSCs).

Materials & Methods: A combination of physical, chemical, and enzymatic treatments was employed for mouse spleen decellularization. These included multiple freeze-thaw cycles, the ionic detergent sodium dodecyl sulfate (SDS), and enzymatic trypsin. Histological and scanning electron microscopy analyses were conducted up to 7 days post-culture to assess the impact of decellularization and cellular adaptation to the spleen scaffolds.

Results: Histological studies revealed the attachment and penetration of BM-MSCs into the scaffolds on days 5-7 following cell seeding. Furthermore, cell migration into the scaffold was observed 5 days after the seeding process.

Conclusion: The decellularization approach utilized in this study proved to be effective and biocompatible, supporting the preservation and proliferation of BM-MSCs. These findings indicate its potential for spleen tissue engineering applications.

Keywords: Decellularization, Scaffold, Spleen tissue, Extracellular matrix, Mesenchymal stem cells

Cite this article: Ghabool Y, Reghbati M, Mahdavi-shahri N, Tavassoli A. Biocompatibility Analysis of Mouse Spleen-Derived ECM. J Adv Biomed Sci. 2024; 14(3): 210-221.
DOI: 10.18502/jabs.v14i3.16358

Introduction

The spleen, primarily populated by cells of the immune system, is characterized by a distinct cellular structure as a secondary lymphatic organ. It plays a crucial role in lymphocyte recycling in rodents and potentially humans (1). Among lymphatic tissues, the spleen is considered the largest lymphatic organ in the human body, uniquely connected to the main circulatory system rather than the lymphatic system. The spleen's functions can be categorized into four main areas: immunity, filtration, hematopoiesis, and storage. While it is an integral part of the immune system, other organs such as the liver and lymph nodes are equally significant (2).

Injuries remain the primary cause of premature death in individuals under 44 years of age, accounting for 12% of the total global disease burden (3). Recent studies have revealed that individuals with coronavirus disease 2019 (COVID-19) or experimental models (SARS-CoV-2) infection can experience splenic organ collapse. In these experimental models, splenic

Corresponding Author: Amin Tavassoli, Division of Biotechnology, Faculty of Veterinary Medicine, Ferdowsi University of Mashhad, Mashhad, Iran.
Email: amin.tavassoli@mail.um.ac.ir, Tavassoli.am@gmail.com

CC BY NC

atrophy and symptomatic lymphopenia were identified (4, 5). The first case reports on splenic function and pathophysiology examined typical causes of organ damage, such as traumatic rupture or malaria-induced infection. Around the turn of the century, the fundamental concepts of hypo- and hypersplenism were introduced, with accumulating data linking splenectomy to an increased risk of infection and thrombosis (6).

To investigate cell-matrix interactions *in vitro*, two key components are required: a suitable cell source and a scaffold. Scaffolds are fundamental to tissue engineering, providing a three-dimensional (3D) framework for cell development *in vitro* (7). They are generally classified into natural and synthetic categories, featuring a porous structure akin to the extracellular matrix (ECM) (8). While numerous synthetic scaffolds have been developed to study cellular behavior in three dimensions, they all exhibit certain limitations, such as an inability to regulate cell adhesion effectively (9).

Tissue engineering presents a potential alternative to overcome the limitations of adverse medicinal approaches. In this context, scaffolds offer an appropriate habitat for various cell behaviors, including differentiation, migration, and growth (2). Decellularized xenografts, due to their unique design characteristics, offer several advantages over other natural and manufactured scaffolds, including a reduction in immunogenic responses while maintaining biological activities (10). Xenogeneic ECM scaffolds have been created from decellularized tissues, including porcine small intestine tendon (11), bladder (12), heart valves (13), and bladder submucosa (14).

The primary component of spleen tissue engineering is a scaffold that provides a 3D environment for cell growth and differentiation, potentially facilitating new tissue formation. Scaffolds fabricated from natural ECM obtained from allografts or xenografts offer advantages over other methods, such as maintaining biological characteristics similar to native tissues. Moreover, the decellularization process leads to a reduction in immune reactions due to the removal of cells and cellular components (15, 16).

Various cellular resources, including malignant, stem, and fibroblastic cells, are commonly employed in cell-matrix interaction studies (17). Mesenchymal stem cells (MSCs) possess the capacity to proliferate effectively *in vitro* and differentiate into various mesenchymal tissues, such as bone, cartilage, fat, and muscle (18). However, a clinical limitation of these cells is their rapid aging and loss of stemness potential following extraction and *in vitro* culture (19).

Decellularization, which involves the elimination of cellular components from the ECM, may therefore prove to be a valuable method for tissue engineering and regenerative medicine applications. The purpose of this study is twofold: to create a decellularized spleen scaffold and to evaluate its cytocompatibility with BALB/c mouse bone marrow-derived mesenchymal stem cells (BM-MSCs).

Materials and Methods

Preparation of spleen tissue

All animal protocols were approved by the Ferdowsi University of Mashhad Animal Research Ethics Committee (Ethical Code: IR.UM.REC.1398.122) prior to implementation. These animal experiments were conducted in accordance with the guidelines of the Iranian Animal Care and Use Council.

Three male BALB/c mice, aged 3 weeks, were procured from the Razi Vaccine and Serum Research Institute in Mashhad, Iran, for spleen tissue preparation. The animals were maintained under standard laboratory conditions. Anesthesia was induced via isoflurane inhalation, after which the spleen tissue was carefully excised through a small incision in the anterior abdominal region of each mouse.

Decellularization Process

The spleen tissue underwent decellularization using a combination of physical, chemical,

and enzymatic processes. For physical decellularization, samples were initially stored at -4°C for one week. Following thawing and washing with normal saline, the tissue underwent five cycles of rapid freezing and thawing in liquid nitrogen.

Trypsin, a proteolytic enzyme commonly employed in decellularization procedures, was utilized to cleave peptide bonds at the carboxyl terminus of amino acids. The extracted spleen tissue was treated with 0.25% trypsin. This endopeptidase degrades proteins into polypeptides, with the aim of eliminating all cells and cellular components while preserving the structure of the ECM and its constituent proteins. To ensure optimal enzyme activity, this complex was incubated at 37°C for one hour (20).

The subsequent stage involved cell eradication via chemical means. To this end, the samples were first subjected to a five-hour wash with an ionic detergent containing sodium dodecyl sulfate (SDS) (Merck, Germany), followed by rinsing with phosphate-buffered saline (PBS). Sterilization was achieved using sterilized distilled water and 75% alcohol. The samples were then rinsed with physiological saline to mitigate any residual effects of the distilled water on the scaffolds. In the final phase, the samples were cultured in Dulbecco's Modified Eagle's Medium (DMEM, Gibco) supplemented with 15% fetal bovine serum (FBS; Gibco) and incubated in Dulbecco's modified eagle's medium (DMEM;Gibco, Brooklyn,NY, USA) at 37°C for 10 minutes in a 5% CO2-air atmosphere (20, 21).

DNA extraction analysis

Genomic DNA was extracted from both normal and decellularized mouse spleen tissue using a commercial kit (Dena Zist Asia, Mashhad, Iran). Following the manufacturer's protocol, 10–15 mg of each tissue sample was processed. The extraction process comprised three key steps: (1) DNA release and binding to the column; (2) column washing; and (3) DNA elution.

Bone marrow-derived mesenchymal stem cells

Mouse BM-MSCs were isolated from the bone marrow of a 1-month-old male Wistar rat. The cells were cultured in 5 ml of DMEM (Gibco, Paisley, Scotland) supplemented with 15% FBS (Gibco, Scotland) and 100 µl penicillin/streptomycin (Biosera, Su, United Kingdom) in a cell culture flask. The culture was maintained in an incubator at 37°C with 5% CO2. After the removal of blood and stromal cells, BM-MSCs were further cultured and purified through trypsinization using 0.25% trypsin/EDTA (22, 23).

Culture of BM-MSCs on Decellularized ECM Derived from Mouse Spleen Tissue

The cell culture medium (DMEM) was supplemented with 10% FBS and 1% penicillin/streptomycin (Pen/Strep). In 24-well flat plates, mesenchymal stem cells isolated from mouse bone marrow were cultured on the ECM scaffold derived from spleen tissue at a density of 10^4 cells per scaffold. Additionally, wells containing cells without scaffolds were designated as "positive controls." On the first, third, fifth, and seventh days following cell implantation, all samples underwent histological staining and were examined using scanning electron microscopy (SEM).

Histological Analysis

Samples were fixed in a 10% formalin solution. Following fixation, they were dehydrated through a graded ethanol series, paraffin-embedded, and transversely sectioned at a thickness of 7 µm using a microtome (Leits, Vienna, Austria). The sections were then deparaffinized with xylene, rehydrated, and stained. A polarized microscope (Olympus, IX70, Japan) was employed to examine sections stained with picrosirius red (Merck, Darmstadt, Germany) for the detection of collagen structures. Hematoxylin and eosin (H&E) staining was utilized to detect cell migration into the 3D scaffold and compare it to control samples. Toluidine blue and safranin O staining were used to demonstrate the presence of proteoglycans and glycosaminoglycans (GAGs)

in decellularized ECM-derived scaffolds.

Fluorescence Microscopy

Fluorescence microscopy was performed using 4',6-Diamidino-2-phenylindole (DAPI), a blue fluorescent dye that preferentially stains dsDNA and firmly binds to adenine and thymine-rich regions (24). The presence of fluorescence on different days of culture on the scaffold may indicate the presence of cells, while the absence of fluorescence on the decellularized scaffold would suggest the absence of cells, as observed under the microscope using the appropriate filters.

Scanning Electron Microscopy

To prepare decellularized and reseeded scaffolds for electron microscopy, samples were fixed with 2.5% glutaraldehyde (TAAB Laboratories, UK) for 24 hours. They were then washed three times for 15 minutes in 0.1 M sodium cacodylate buffer (TAAB Laboratories, UK). Subsequently, the samples underwent a 1-hour treatment with 1% osmium tetroxide (TAAB Laboratories, UK), followed by a second wash in 0.1 M sodium cacodylate buffer and dehydration using a graded ethanol series. Finally, the scaffolds were mounted on metal supports and sputter-coated with gold-palladium (Sputter Coater, SC7620, East Sussex, UK) before examination using a SEM (LEO 1450VP, Germany).

Results

The results of this research are presented in two sections: scaffold fabrication, which involves the production of ECM from mouse spleen, and the *in vitro* interaction between cells extracted from mouse bone marrow and decellularized spleen tissue. A physicochemical technique was employed to decellularize spleen tissue, which was subsequently analyzed histologically to determine its characteristics.

The histological effects of these methods on decellularized spleen tissue were examined. H&E staining of non-decellularized and decellularized tissue demonstrated the complete decellularization of spleen tissue. Post-decellularization, microscopic images using various dyes revealed the absence of cells in the spleen tissue compared to its initial, non-decellularized state.

Examination of the decellularized spleen tissue with H&E staining showed that the samples were completely devoid of cells, with nuclei having been removed from the spleen tissue compared to the control sample (Figures 1A and 1B).

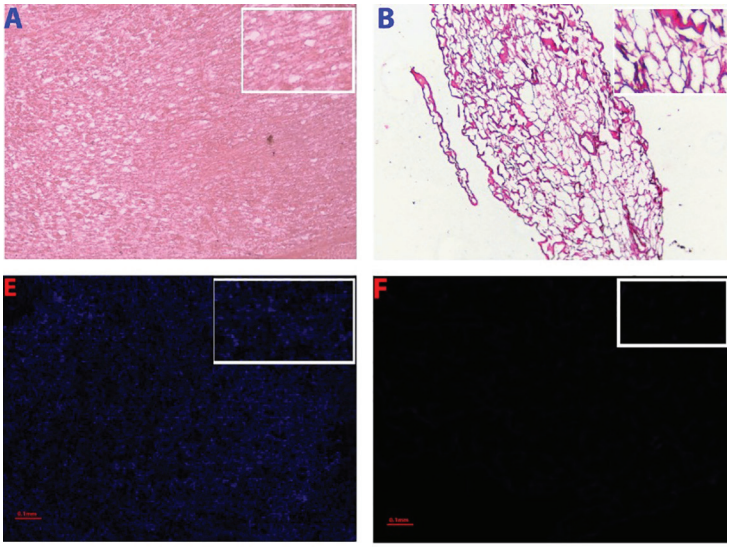


Figure 1. A) Spleen tissue with cells and reticular filaments; B) H&E staining demonstrating complete removal of cell nuclei post-decellularization; C) DAPI fluorescent labeling revealing numerous spleen cells in the tissue; D) Absence of fluorescence signifying cell removal and nucleic acid disruption, thus demonstrating the decellularization procedure's efficacy.

DAPI staining was employed to further demonstrate the removal of nuclei from spleen tissue scaffolds. The findings confirmed that cells were entirely removed from the scaffold using the specified approach (Figures 1C and 1D).

Consistent with these findings, SEM micrographs revealed no traces of cells or cell fragments in the ECM network following the decellularization procedure, whereas cells were visible in control samples (Figures 2A and 2B).

The efficacy of decellularization and retention of ECM components were assessed through DNA extraction analysis (Figure 3) and histological examinations as described above. The results of H&E staining, DAPI fluorescence, SEM micrographs, and DNA analysis collectively indicated successful removal of cellular materials while maintaining relatively good preservation of the ECM structure.

Analysis of BM-MSCs on the Decellularized Spleen Tissue Scaffold at Days 1, 3, 5, and 7 Post-Culture

Several cultured tissues were stained during a 24-hour incubation period. As indicated by the arrow in Figure 4A, the spots on the scaffold in the H&E-stained image suggest the presence of viable seeded cells. Histological examinations using H&E staining revealed a significant increase in the number of cells attached to the scaffolds by the third day of culture. Cell aggregates formed at specific locations, arranged in continuous layers, with some cells migrating into the inner regions of the scaffold (Figure 4B). By the fifth day of culture, analysis exhibited a reduction in cell accumulation on the scaffold compared to the third day, with cells showing a tendency to penetrate the scaffold (Figure 4C). The percentage of spleen scaffold area covered by mouse BM-MSCs reached its maximum on day 7 of culture (Figure 4D).

Toluidine blue staining, which qualitatively shows the distribution of sulfated proteoglycans in the ECM, revealed that these components initially disappeared from the media following re-cellularization. However, the toluidine blue stain developed 5 and 7 days after culture, indicating sulfated proteoglycan reconstitution (Figure 5).

DAPI staining on day 1 revealed brighter spots, indicating the survival and adherence of BM-MSCs to the spleen ECM scaffold (Figure 6A). Subsequent DAPI staining showed an increase in cell numbers and their penetration into the scaffold (Figure 6B). By day 5, increased cell migration compared to previous days, as well as a tendency to infiltrate the scaffold, was observed (Figure 6C).

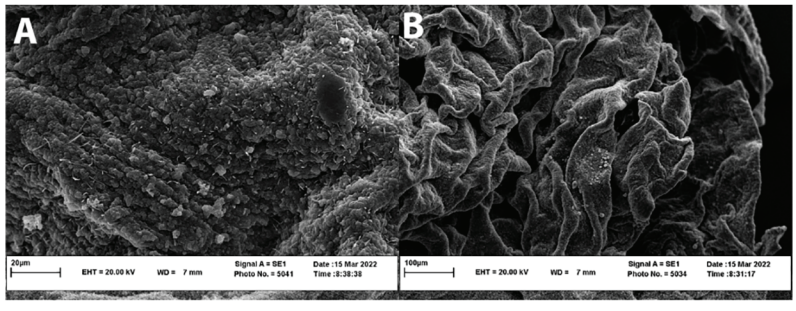


Figure 2. SEM images of BALB/c mouse spleen: A) Control sample showing visible cells, corroborating light and fluorescence microscopy findings; B) Decellularized scaffold displaying no traces of cells or cell fragments throughout the ECM network, with closely aligned collagen fibers.



Figure 3. DNA extraction analysis display of normal and decellularized mouse spleen tissue

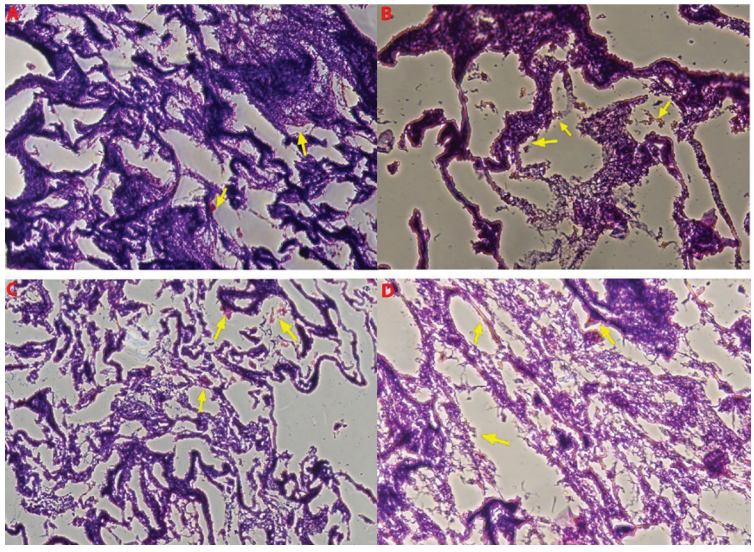


Figure 4. Representative H&E stained images of cells transplanted on the spleen tissue matrix at various time intervals: A) & B) Low density of BM-MSCs in the splenic matrix after 1 and 3 days of culture, respectively; C) & D) Increased cell adhesion and penetration after 5 and 7 days of cultivation. Arrows indicate spots on the scaffold suggesting viable seeded cells.

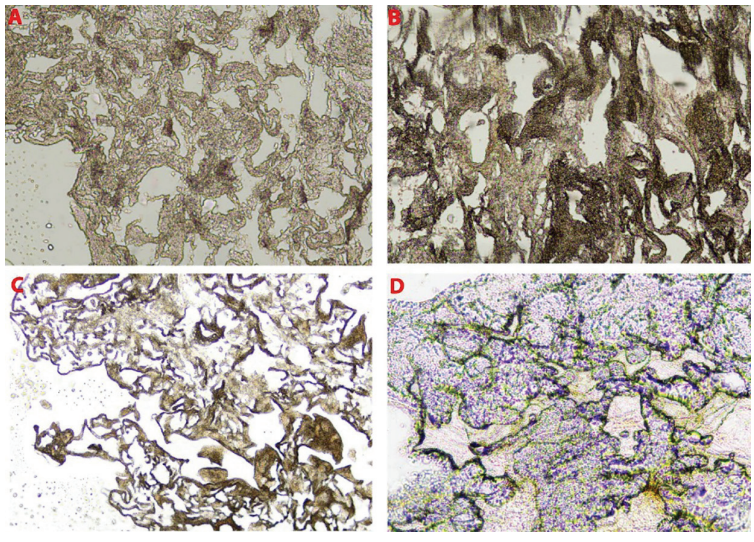


Figure 5. Qualitative assessment of sulfated proteoglycan distribution in the ECM via toluidine blue staining: A) & B) Absence of staining at 1 and 3 days post-culture; C) & D) Toluidine blue stain formation at 5 and 7 days post-culture, indicating sulfated proteoglycan reconstitution.

On the seventh day of culture, DAPI staining revealed that the scaffold effectively supported cell maintenance and transformation, facilitating the formation of a basal layer and an increase in primary cell mass density (Figure 6D).

SEM findings on the third day of culture indicated mass adhesion of cells with active nuclei and the presence of cell-like formations (Figure 7A). By day 5, SEM observations revealed cells with reduced density and altered shape, as well as evidence of attempts to penetrate the scaffold (Figure 7B).

Discussion

Prior to this study, numerous investigations had been conducted in the realm of developing organic scaffolds. However, this particular research set out to achieve its objective of creating

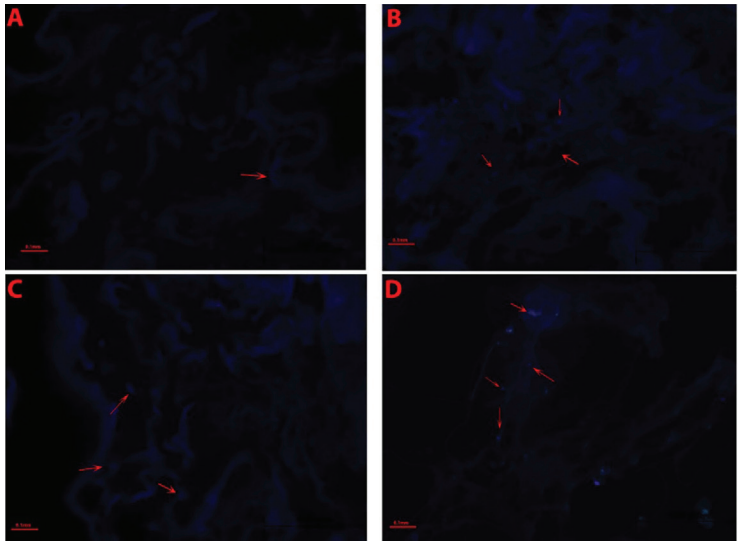


Figure 6. DAPI staining of BM-MSCs on spleen scaffolds at various stages of growth: A) Bright nuclei evident on the scaffold surface one day post-cell implantation; B) Increased presence of bright nuclei surrounding the scaffolds on day 3; C) & D) Penetration of bright nuclei into the scaffolds observed during culture durations of 5 and 7 days, respectively.

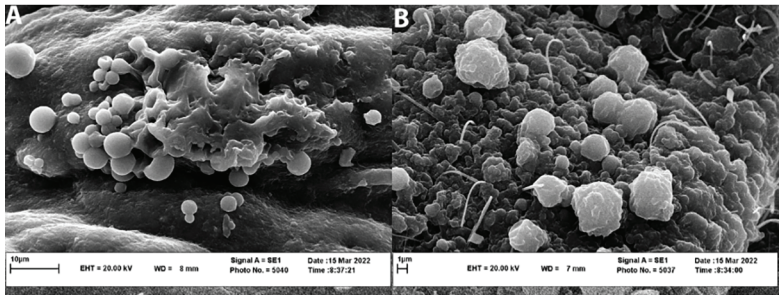


Figure 7. SEM images of spleen scaffolds seeded with BM-MSCs: A) Mass of cells attached to the scaffold on the third day of cell culture; B) Increased maintenance and adhesion of BM-MSCs on the spleen scaffold after seven days of cultivation.

a durable structure for enhanced maintenance and adhesion by implementing a novel protocol for tissue decellularization. Based on the results presented, it can be inferred that this scaffold has successfully established favorable compatibility BM-MSCs and the decellularized spleen tissue scaffold.

Most studies have utilized the decellularized matrix of the spleen as a scaffold to restore liver and pancreatic functions (25, 26). In the analysis of cell migration, using models based on experimental reality may be both controversial and valuable. Generally, two-dimensional cell culture or animal model evaluation contributes to our understanding of cell interactions ECM. However, animal models, often used in definitive experiments, cannot reproduce certain aspects of cell migration, drug response, tumor metastasis, autoimmune disorders, and stem cell differentiation processes (21). Consequently, 3D cell culture in the laboratory may create a comparable cell culture environment to animal models, thereby providing a more appropriate analysis (21).

Various decellularization methods have been developed for several relevant tissues, such as blood vessels (27), heart valves (28), small intestine submucosa (29), skin (30), tendons, and ligaments (31). In contrast to synthetic scaffolds, decellularized tissues provide natural scaffolds

that maintain the structure of the native ECM. By preserving the components of the tissue matrix, they enhance migration, cell adhesion, and cell growth (32, 33).

In this study, chemical decellularization was employed in addition to physical and enzymatic techniques. H&E staining and SEM findings were used to demonstrate the removal of cellular components from the scaffold. Research has indicated that the removal of DNA presents a greater challenge compared to other intracellular substances due to its propensity to adhere to ECM proteins (34). Residual DNA after decellularization may cause inflammatory responses following implantation (35). Apart from DNA, other cellular components, such as lipids and cellular proteoglycans, can also trigger an immune response (36).

DAPI staining and DNA extraction analysis confirmed the complete removal of DNA from the decellularized spleen tissue. In several prior studiesSDS has shown remarkable decellularization capacities by eliminating cellular debris while maintaining ECM components and strength (20). For instance, this detergent has proven more successful in decellularizing tissues such as adult pig kidney, sheep esophagus, bovine pericardium, and articular cartilage (20).

Although decellularized scaffolds have been successfully created from multiple organs and tissues, there is no universally applicable method for decellularizing all tissues. The appropriate protocol is determined by various factors, including tissue type, species, age, size, and anatomical location. Consequently, in several studies, an optimal protocol was devised by combining decellularization approaches such as chemical, physical, and enzymatic treatments with different agents (37).

Studies have shown that tissues treated with detergents after rapid freeze-thaw cycles lose their cellular components more effectively (38, 39). While cells and cellular proteins are destroyed by freeze-thaw cycles, other cellular components, such as the nucleus, are not eliminated by this process alone; treatment with various detergents is necessary to remove cellular compounds entirely (39). According to Elder et al. (15, 40), greater decellularization was achieved when a detergent was used in addition to freeze-thaw cycles.

Research has demonstrated that SDS does not diminish the stiffness of decellularized tissues while retaining ECM molecules (12). Histological examinations in this study have shown that a concentration of 2% SDS for 5 hours yields the most significant cell elimination results. Higher concentrations of SDS, on the other hand, remove essential proteins from the splenic matrix. SDS may interact with the cell membrane and induce cell membrane and nuclear membrane lysis due to its dual structure. SDS has been reported to be more effective than Triton X-100 for removing cells in the medullary regions of dense organs and preserving the spleen's internal architecture (41).

Collagen and laminin play crucial roles in cell regeneration, proliferation, migration, restoration of normal function, and organ regeneration after injury (42). Collagen, the primary component of the ECM, is important in biomechanics, facilitating the transfer of tissue forces to cells (43). During tissue repair processes, collagen also affects cell phenotype and performs local growth factor and cytokine storage and release functions (44). One of the most significant roles of the ECM is to act as an adhesive substrate for cell migration. This substrate contains essential chemicals as well as natural fibers such as collagen and reticular fibers. Various components of the ECM may have different effects on cell adhesion and migration speed (45).

Other significant components in the ECM include laminins, which are responsible for cell adhesion (46), regulation of cell migration, and differentiation (47), as well as glycosaminoglycans. These components are maintained following decellularization.

Several matrix components, including laminin, fibronectin, and collagens, are required to maintain the structure of the spleen's basement membrane and interstitial matrices (48, 49). Several studies have shown that collagen subtypes in the ECM mimic those of normal tissues after decellularization (24, 50).

According to SEM analysis, the decellularized spleen scaffolds were well-structured to promote cell migration, differentiation, and the transfer of nutrients and waste products during cell culture. On days 3 and 7 after mouse BM-MSCs were cultured on the decellularized scaffold, cell maintenance was assessed. SEM photographs demonstrated the effective attachment of cells to the collagen and reticular fibers of the spleen five days after culture. The distribution of sulfated proteoglycans in the ECM, qualitatively shown by toluidine blue staining, initially disappeared from the surrounding area following re-cellularization. However, the toluidine blue color reappeared on days 5 and 7 after culture, demonstrating the regeneration of sulfated proteoglycans. These results indicate that cell attachment and maintenance can occur on a scaffold created from cell-free spleen tissue using physical, chemical, and enzymatic decellularization techniques.

In conclusion, this scaffold represents a potential future platform for spleen tissue engineering, and its use with other differentiable stem cells supports critical tasks such as attachment and differentiation. However, further research is required to assess the potential immunological response of host tissue to this decellularized scaffold, as well as its potential use in animal models with agents such as spleen morphogenetic proteins like fibronectin. Overall, our findings support the use of 3D cell culture *in vitro*. This approach could serve as a promising xenograft model for the repair of spleen and liver abnormalities in humans, but further *in vivo* research is necessary to validate this claim.

Conclusion

This study's findings encompass data analysis and the creation of a 3D scaffold using decellularization techniques from mouse spleen ECM. Furthermore, the study utilized mesenchymal stem cells derived from bone marrow and examined their interaction with the decellularized spleen matrix as a model to investigate cell behavior under various tissue conditions. Visible adhesion, proliferation, and polarity were observed in the subjects. Additional research could be conducted by enhancing the ECM with key proteins involved in differentiation, such as fibronectin, to achieve more accurate modeling.

Acknowledgment

We express our sincere appreciation to Dr. Jina Khayatzadeh of the Islamic Azad University of Mashhad branch for her insightful discussions. We would also like to extend our gratitude to Dr. Fatemeh Nasseri for her outstanding technical assistance with electron microscopy.

Conflict of interest

The authors declare no conflict of interest.

Ethical Consideration

The ethical approval for this study was issued by the Ethics Committee of the Ferdowsi University of Mashhad, in accordance with the Ethical Guidelines of the Ministry of Science, Research and Technology of Iran and the Declaration of Helsinki.

Code of Ethics

Ethics Committee of the Ferdowsi University of Mashhad: IR.UM.REC.1398.122.

Authors Contributions

Conception and design of the study: NMS and AT Performance of the experiments: YG and MR Data analysis: YG, MR, and AT Supervision of the study: NMS Drafting of the manuscript:

YG, MR, and AT. All authors read and approved the final version of the manuscript.

Availability of Data and Materials

Datasets used and/or analyzed during the current study are available from the corresponding author upon reasonable request.

Code availability

Not applicable.

Consent for Publication

No patient-identifiable information is included in this report.

References

1 Steiniger BS. Human spleen microanatomy: why mice do not suffice. Immunology. 2015;145(3):334-46.
2 Cadili A, de Gara C. Complications of splenectomy. Am J Med. 2008;121(5):371-5.
3 Cesta MF. Normal structure, function, and histology of the spleen. Toxicol Pathol. 2006;34(5):455-65.
4 Chan JF, Zhang AJ, Yuan S, Poon VK, Chan CC, Lee AC, et al. Simulation of the Clinical and Pathological Manifestations of Coronavirus Disease 2019 (COVID-19) in a Golden Syrian Hamster Model: Implications for Disease Pathogenesis and Transmissibility. Clin Infect Dis. 2020;71(9):2428-46.
5 Xu X, Chang XN, Pan HX, Su H, Huang B, Yang M, et al. Pathological changes of the spleen in ten patients with coronavirus disease 2019(COVID-19) by postmortem needle autopsy. Zhonghua Bing Li Xue Za Zhi. 2020;49(6):576-82.
6 Riva MA, Ferraina F, Paleari A, Lenti MV, Di Sabatino A. From sadness to stiffness: the spleen's progress. Intern Emerg Med. 2019;14(5):739-43.
7 Saxena AK. Tissue engineering and regenerative medicine research perspectives for pediatric surgery. Pediatr Surg Int. 2010;26(6):557-73.
8 Walker C, Mojares E, Del Río Hernández A. Role of extracellular matrix in development and cancer progression. Int J Mol Sci. 2018 Oct 4;19(10):3028.
9 Friedl P, Wolf K. Tumour-cell invasion and migration: diversity and escape mechanisms. Nat Rev Cancer. 2003;3(5):362-74.
10 Shahabipour F, Mahdavi-Shahri N, Matin MM, Tavassoli A, Zebarjad SM. Scaffolds derived from cancellous bovine bone support mesenchymal stem cells' maintenance and growth. In Vitro Cell Dev Biol Anim. 2013;49(6):440-8.
11 Cartmell JS, Dunn MG. Effect of chemical treatments on tendon cellularity and mechanical properties. J Biomed Mater Res. 2000;49(1):134-40.
12 Rosario DJ, Reilly GC, Ali Salah E, Glover M, Bullock AJ, Macneil S. Decellularization and sterilization of porcine urinary bladder matrix for tissue engineering in the lower urinary tract. Regen Med. 2008;3(2):145-56.
13 Liao J, Joyce EM, Sacks MS. Effects of decellularization on the mechanical and structural properties of the porcine aortic valve leaflet. Biomaterials. 2008;29(8):1065-74.
14 Gilbert TW, Stolz DB, Biancaniello F, Simmons-Byrd A, Badylak SF. Production and characterization of ECM powder: implications for tissue engineering applications. Biomaterials. 2005;26(12):1431-5.
15 Elder BD, Eleswarapu SV, Athanasiou KA. Extraction techniques for the decellularization of tissue engineered articular cartilage constructs. Biomaterials. 2009;30(22):3749-56.
16 Hoshiba T, Chen G, Endo C, Maruyama H, Wakui M, Nemoto E, et al. Decellularized Extracellular Matrix as an In Vitro Model to Study the Comprehensive Roles of the ECM in Stem Cell Differentiation. Stem Cells Int. 2016;2016:6397820.
17 Corcoran JP, Ferretti P. RA regulation of keratin expression and myogenesis suggests different ways of regenerating muscle in adult amphibian limbs. J Cell Sci. 1999;112 (Pt 9):1385-94.
18 Rozario T, DeSimone DW. The extracellular matrix in development and morphogenesis: a dynamic view. Dev Biol. 2010;341(1):126-40.
19 Bonab MM, Alimoghaddam K, Talebian F, Ghaffari SH, Ghavamzadeh A, Nikbin B. Aging of mesenchymal stem cell in vitro. BMC Cell Biol. 2006;7:14.
20 Khakpour E, Tavassoli A, Mahdavi-Shahri N, Matin MM. Assessing the biocompatibility of bovine tendon scaffold, a step forward in tendon tissue engineering. Cell Tissue Bank. 2022;23(3):439-49.
21 Kohannezhad K, Norouzi S, Tafazoli M, Soleymani S, Shahri NM, Tavassoli A. The in vitro analysis of migration and polarity of blastema cells in the extracellular matrix derived from bovine mesenteric in the presence of fibronectin. Anat Cell Biol. 2022;55(2):229-38.
22 Ghasroldasht MM, Irfan-Maqsood M, Matin MM, Bidkhori HR, Naderi-Meshkin H, Moradi A, et al. Mesenchymal stem cell based therapy for osteodiseases. Cell Biol Int. 2014;38(10):1081-5.
23 Neshati Z, Matin MM, Bahrami AR, Moghimi A. Differentiation of mesenchymal stem cells to

insulin-producing cells and their impact on type 1 diabetic rats. J Physiol Biochem. 2010;66(2):181-7.
24 Atale N, Gupta S, Yadav UC, Rani V. Cell-death assessment by fluorescent and nonfluorescent cytosolic and nuclear staining techniques. J Microsc. 2014;255(1):7-19.
25 Vishwakarma SK, Lakkireddy C, Bardia A, Nagarapu R, Paspala SAB, Habeeb MA, et al. Biofabricated Humanized Insulin Producing Neo-Organs Generates Secondary Neo-Organoids Through Ectopic Transplantation. Cellular and Molecular Bioengineering. 2019;12(6):569-82.
26 Xiang JX, Zheng XL, Gao R, Wu WQ, Zhu XL, Li JH, et al. Liver regeneration using decellularized splenic scaffold: a novel approach in tissue engineering. Hepatobiliary Pancreat Dis Int. 2015;14(5):502-8.
27 Schmidt CE, Baier JM. Acellular vascular tissues: natural biomaterials for tissue repair and tissue engineering. Biomaterials. 2000;21(22):2215-31.
28 Schenke-Layland K, Vasilevski O, Opitz F, Konig K, Riemann I, Halbhuber KJ, et al. Impact of decellularization of xenogeneic tissue on extracellular matrix integrity for tissue engineering of heart valves. J Struct Biol. 2003;143(3):201-8.
29 Kropp BP, Eppley BL, Prevel CD, Rippy MK, Harruff RC, Badylak SF, et al. Experimental assessment of small intestinal submucosa as a bladder wall substitute. Urology. 1995;46(3):396-400.
30 Chen RN, Ho HO, Tsai YT, Sheu MT. Process development of an acellular dermal matrix (ADM) for biomedical applications. Biomaterials. 2004;25(13):2679-86.
31 Woods T, Gratzer PF. Effectiveness of three extraction techniques in the development of a decellularized bone-anterior cruciate ligament-bone graft. Biomaterials. 2005;26(35):7339-49.
32 Rafighdoust A, Shahri NM, Baharara J. Decellularized kidney in the presence of chondroitin sulfate as a natural 3D scaffold for stem cells. Iran J Basic Med Sci. 2015;18(8):788-98.
33 Nakayama KH, Batchelder CA, Lee CI, Tarantal AF. Renal tissue engineering with decellularized rhesus monkey kidneys: age-related differences. Tissue Eng Part A. 2011;17(23-24):2891-901.
34 Ross JR, Kirk AD, Ibrahim SE, Howell DN, Baldwin WM, 3rd, Sanfilippo FP. Characterization of human anti-porcine "natural antibodies" recovered from ex vivo perfused hearts--predominance of IgM and IgG2. Transplantation. 1993;55(5):1144-50.
35 Gilbert TW, Sellaro TL, Badylak SF. Decellularization of tissues and organs. Biomaterials. 2006;27(19):3675-83.
36 Nagata S, Hanayama R, Kawane K. Autoimmunity and the clearance of dead cells. Cell. 2010;140(5):619-30.
37 Zhang X, Chen X, Hong H, Hu R, Liu J, Liu C. Decellularized extracellular matrix scaffolds: Recent trends and emerging strategies in tissue engineering. Bioact Mater. 2022;10:15-31.
38 Stapleton TW, Ingram J, Katta J, Knight R, Korossis S, Fisher J, et al. Development and characterization of an acellular porcine medial meniscus for use in tissue engineering. Tissue Eng Part A. 2008;14(4):505-18.
39 Murphy CM, Matsiko A, Haugh MG, Gleeson JP, O'Brien FJ. Mesenchymal stem cell fate is regulated by the composition and mechanical properties of collagen-glycosaminoglycan scaffolds. J Mech Behav Biomed Mater. 2012;11:53-62.
40 Elder BD, Kim DH, Athanasiou KA. Developing an articular cartilage decellularization process toward facet joint cartilage replacement. Neurosurgery. 2010;66(4):722-7; discussion 7.
41 Nakayama KH, Batchelder CA, Lee CI, Tarantal AF. Decellularized rhesus monkey kidney as a three-dimensional scaffold for renal tissue engineering. Tissue Eng Part A. 2010;16(7):2207-16.
42 Walker PD. Alterations in renal tubular extracellular matrix components after ischemia-reperfusion injury to the kidney. Lab Invest. 1994;70(3):339-45.
43 Walker C, Mojares E, Del Río Hernández A. Role of Extracellular Matrix in Development and Cancer Progression. Int J Mol Sci. 2018;19(10):3028.
44 Miranda-Nieves D, Chaikof EL. Collagen and Elastin Biomaterials for the Fabrication of Engineered Living Tissues. ACS Biomater Sci Eng. 2017;3(5):694-711.
45 Strachan LR, Condic ML. Neural crest motility and integrin regulation are distinct in cranial and trunk populations. Dev Biol. 2003;259(2):288-302.
46 Nara S, Chameettachal S, Midha S, Murab S, Ghosh S. Preservation of biomacromolecular composition and ultrastructure of a decellularized cornea using a perfusion bioreactor. RSC advances. 2016;6(3):2225-40.
47 Mouw JK, Ou G, Weaver VM. Extracellular matrix assembly: a multiscale deconstruction. Nat Rev Mol Cell Biol. 2014;15(12):771-85.
48 Lokmic Z, Lämmermann T, Sixt M, Cardell S, Hallmann R, Sorokin L, editors. The extracellular matrix of the spleen as a potential organizer of immune cell compartments. Seminars Immunol. 2008: Elsevier.
49 Zanardo TEC, Amorim FG, Taufner GH, Pereira

RHA, Baiense IM, Destefani AC, et al. Decellularized Splenic Matrix as a Scaffold for Spleen Bioengineering. Front Bioeng Biotechnol. 2020;8:573461.
50 Sackett SD, Tremmel DM, Ma F, Feeney AK, Maguire RM, Brown ME, et al. Extracellular matrix scaffold and hydrogel derived from decellularized and delipidized human pancreas. Sci Rep. 2018;8(1):10452.